Proceedings of the 5th International Conference on Advances in Energy Research and Applications (ICAERA 2024)
Lisbon, Portugal- November 21 - 23, 2024
Paper No. 135
DOI: 10.11159/icaera24.135

Thermal Management Of Highly Concentrated Photovoltaic-Thermal System Using Confined Jet Impingement And Thermoelectric Generator

Abhishek Gupta[1], Sandesh S. Chougule[2], Sandip K. Saha[1]
[1]Department of Mechanical Engineering, Indian Institute of Technology Bombay
Mumbai - 400076, India
204100029@iitb.ac.in; s.chougule@imperial.ac.uk
[2]Clean Energy Processes (CEP) Laboratory, Department of Chemical Engineering, Imperial College London
London SW72AZ, United Kingdom
sandip.saha@iitb.ac.in

Abstract **-** The high concentration of solar light on photovoltaic cells leads to extremely high cell temperatures, which leads to decreased cell electrical efficiency. Appropriate cooling techniques need to be integrated to maintain the PV cell temperature within the permissible temperature limit. The present study focuses on the cooling of the highly-concentrated photovoltaic thermal system using a confined jet impingement cooling system and a thermoelectric generator. The proposed configuration generates electrical power from the waste heat. The thermoelectric generator is placed between the solar cell layers and the aluminium heat sink. The effect of different TEG module sizes on the power generated by the system has been studied. The total power generated by the hybrid system is maximum with a 25×25 mm TEG module. The present study will be useful in the thermal management of highly concentrated photovoltaic thermal systems.

Keywords**:** Concentrated photovoltaic; confined jet impingement; thermoelectric generator; efficiency; power

1. Introduction

Solar energy can be used by various technologies, such as photovoltaic (PV) systems, solar thermal collectors, and concentrated photovoltaic (CPV) systems. PV systems and solar thermal collectors can be integrated to produce electrical and thermal energy outputs simultaneously. PV-T systems can expand solar energy utilisation by improving cell conversion efficiency. Concentrated photovoltaic thermal (CPV-T) systems can be used to obtain thermal energy at a high temperature since flat plate PV-T systems generate heat energy at a very low temperature.

CPV-T system uses optics to concentrate the solar radiation on the PV cell surface. Despite the many advantages of CPV-T systems over flat plate PV-T systems, CPV-T systems face many challenges. The highly concentrated solar radiation on the PV cell surface results in an increased cell temperature, which results in a decrease in cell electrical efficiency. This leads to major problems such as thermal hotspots, current mismatching, and thermal fatigue of the solar PV cell. Hence, appropriate cooling techniques are required to cool the PV cell at high concentrations.

Many cooling techniques, such as passive cooling, liquid immersion cooling, PCM cooling, microchannel cooling, jet impingement cooling, and thermoelectric cooling, have been studied in various literature[1]. Theristis et al. [2] reported that passive cooling methods could not remove sufficient heat from the PV cells under high concentration ratios. The jet impingement cooling technique is an appropriate method for the cooling of densely packed PV cells[3]. Many researchers have studied unconfined and confined jet impingement cooling techniques. Javidan et al. [4] observed a reduction in cell temperature from 63.95 °C to 33.68 °C using an optimal set of multi-nozzle jet impingement configurations. Bahaidarah et al. [5] observed a decrease in cell temperature from 69.7 °C to 36.6 °C using 8 nozzles of diameter 5 mm with jet impingement cooling. Abo-Zahhad et al. [6] observed a reduction in cell temperature from 1360 °C to 65 °C at a concentration ratio of 1000 with water at a mass flow rate of 50 g/min. Tang et al. [7] studied the effect of the ultrathin micro pin-fin channel on the performance of the HCPV-T system under CR = 1000 and observed a cell temperature of 51°C at a mass flow rate of 3 kg/h. Shohdy et al. [8] observed the effect of the microchannel and trimmed fins on the performance of the HCPV-T system under CR = 2500 and observed that the cell temperature was reduced by 88.68 °C with a hybrid heat sink. Sabry et al. [9]

studied the thermoelectric generator (TEG) cooling of concentrated PV systems. The generated power of the CPV/TEG hybrid system was increased by 7.4%, 5.8%, and 3%, corresponding to 30 × 30 mm^2, 40 × 40 mm^2, and 62 × 62 mm^2 TEG modules. Kohan et al. [10] studied the effect of TEG cooling on the backside of the PV cell. The author observed that the hybrid PV/TEG system can generate more power than the PV system alone. However, the difference in the power generation was found to be marginal due to insufficient temperature difference between hot and cold junctions of TEG.

It can be concluded from the literature that CPV/TEG systems can generate more electrical power than conventional CPV systems alone. However, the power generated by the TEG module depends on the temperature difference between the hot and cold junction temperatures of the TEG module. The current study aims to use hybrid cooling, i.e. confined jet impingement and thermoelectric generator, to improve the overall performance of the HCPV-T system. The hot junction of the TEG module is attached to the PV cell layer, and the cold junction of the TEG module is attached to the confined jet impingement. It leads to the maximum temperature difference between the two junctions of the TEG module. The effect of the coolant mass flow rate on the overall performance of the hybrid system has been studied. Also, the effect of the TEG module area on the overall power generation by the hybrid system has been observed.

2. System description:

The HCPV-T system consists of a solar cell with a direct bond copper (DBC) assembly. The solar cell used in this study is a multi-junction solar cell with a reference cell electrical efficiency of 40.3% at a reference temperature of 298 K [11]. An aluminium heat sink is placed at the bottom part of the DBC assembly. The channels are created inside the aluminium heat sink such that the cooling fluid strikes the heat sink surface at the centre and leaves from the four outlets at the corner. A thermoelectric generator is placed between the DBC assembly and the aluminium heat sink. The HCPV-T system is shown in Figure 1. Three distinct sizes of TEG modules are used in this study.

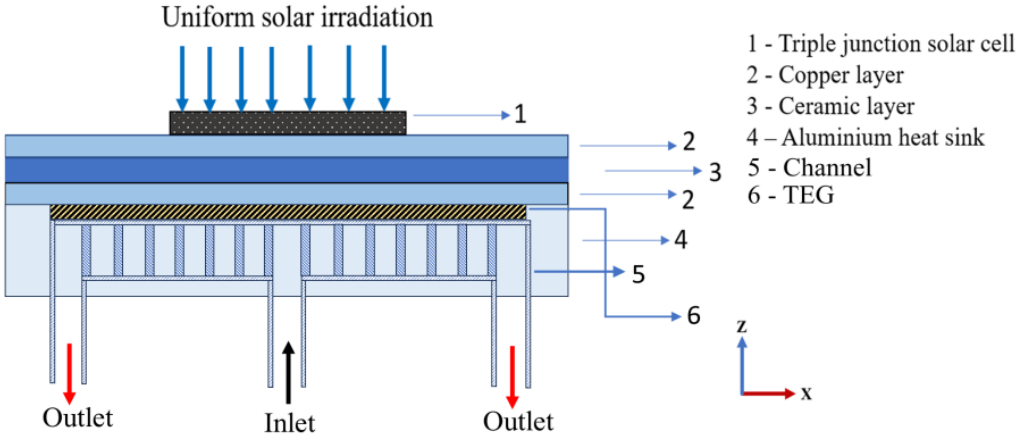

Figure 1. HCPV-T system with confined jet impingement and thermoelectric generator

The dimensions and thermophysical properties of the solar cell and layers are given in Tables 1 and 2, respectively.

Table 1. Dimensions of the solar cell, DBC assembly, and heat sink

Layer	Thickness (mm)	Length (mm)	Width (mm)
Germanium	0.19	10	10
Copper-1 and 2	0.25	25	25
Ceramic	0.32	25	25
Aluminium heat sink	4	25	25
TEG module	1	15, 20, 25	15, 20, 25

Table 2. Thermophysical properties of the solar cell, DBC assembly, heat sink, and TEG [12]

Layer	Thermal conductivity (k) (W/m·K)	Specific heat (C_p) (J/kg·K)	Density (ρ) (kg/m^3)	Emissivity (ε)
Germanium	60	320	5323	0.9
Copper	400	385	8700	0.05
Ceramic	30	900	3900	0.75
Aluminium	202.6	871	2719	0.9
TEG module (Bismuth-Telluride)	1.45	550	4100	0.66
Coolant fluid (water)	0.6	4182	998	-

3. Governing equations:

3.1 For solar cell layers

The heat conduction equation between the layers of the PV cell is as follows:

$$k_i \nabla^2 T_i + q_i = 0 \quad (1)$$

where, k_i denotes the thermal conductivity of the i^{th} layer. In all layers except the Ge layer, the heat generation, q_i is set to zero. The heat generated due to solar radiation absorption in the Ge layer is estimated as:

$$q_{Ge} = \frac{\left(1 - \eta_{cell}\right) \cdot G \cdot \alpha_{Ge} \cdot A}{V} \quad (2)$$

where G is the net concentrated solar radiation on the solar cell surface. α_{Ge} represents the absorptivity of the germanium layer. A and V represent the surface area and volume of the PV cell, respectively. η_{cell} denotes the electrical efficiency of the cell.

The net concentrated solar radiation is given as:

$$G = I \cdot CR \cdot \eta_{opt} \quad (3)$$

where I is the solar irradiation falling on the solar cell. I is taken as 1000 W/m^2 and is assumed to be uniformly distributed on the PV cell surface. CR is the concentration ratio, and η_{opt} is the optical efficiency of the solar cell. The optical efficiency of the PV cell is taken as 0.9.

The electrical efficiency of the solar cell (η_{cell}) is a function of the temperature of the solar cell. It is expressed using the following equation:

$$\eta_{cell} = \eta_{ref} - \beta_T (T_{cell} - T_{ref}) \quad (4)$$

where, cell reference efficiency η_{ref} is taken as 40.3% at reference temperature T_{ref} = 298 K and CR = 1000, and β_T is the thermal coefficient and is considered as 0.047% [11].

The total electric power generated by the PV cell can be calculated as:

$$P_{el} = \eta_{cell} \cdot G \cdot \alpha_{Ge} \cdot A \quad (5)$$

3.2 For flow and heat transfer through jet impingement:

The flow is assumed to be steady and incompressible. The thermophysical properties are taken as isotropic and temperature-independent. The fluid flow is considered as Newtonian.

Continuity equation: $$\rho_f (\vec{V}) = 0 \quad (6)$$

Momentum equation: $$\rho_f (\vec{V}.\ \vec{V}) = -P + \mu^2\ \vec{V} \quad (7)$$

Energy equation: $$\rho_f C_{p,f} (\vec{V}.\ T) = k_f^2 T \quad (8)$$

where, ρ_f and μ are the coolant density and coolant viscosity, and k_f represents the thermal conductivity of the coolant. $\vec{V}$ is coolant velocity, and P is the pressure.

3.3 For TEG model

The temperature distribution in the TEG is modelled as:

$$k\nabla^2 T - P_{gen} = 0 \tag{9}$$

where, P_{gen} is the power generated per unit volume by the TEG module.

The power generated by the TEG module can be estimated as [13]:

$$P_{TEG} = n \cdot \epsilon_t \cdot I_g \cdot \left(T_h - T_c\right) + I_g{}^2 R \tag{10}$$

where, n is the number of p-n units in the TEG module. The number of p-n units in the TEG module is taken as 128. ε_t is the mean Seeback coefficient of the TEG module. The Seeback coefficient of the TEG module is taken as 282 μV/K [14]. T_h and T_c are the temperatures of the hot and cold junction of the TEG module, respectively. I_g is the electric current in TEG, and R is the electrical resistance of the TEG module.

The electric current and electrical resistance of the TEG module can be calculated using the following equation [13][14].

$$I_g = \frac{n \cdot \varepsilon_t \cdot (T_h - T_c)}{R(1+\mu)} \tag{11}$$

$$R = 10^{-5} \times (-3)\left(T_m - 273\right)^2 - 0.0133\left(T_m - 273\right) + 1.542 \tag{12}$$

where, T_m is the mean temperature of the hot and cold junction temperature of the TEG module.

4. Boundary conditions

The upper surface of the PV cell and the copper layer are subjected to convective and radiative boundary conditions. All sides of the PV cell, DBC assembly, and heat sink are subjected to convective boundary conditions. All the interfaces are given thermally coupled boundary conditions. Uniform temperature and normal velocity boundary conditions are given at the coolant inlet. Zero-gauge pressure condition is given at the coolant outlet. For the upper surface of the PV cell and top copper layer:

$$-k_{Ge}\frac{\partial T_{Ge}}{\partial z} = q_{rad,Ge\to S} + q_{conv,Ge\to a} \tag{13}$$

$$-k_{cu}\frac{\partial T_{cu}}{\partial z} = q_{rad,cu\to S} + q_{conv,cu\to a} \tag{14}$$

where, $q_{rad,Ge\to S}$ is the radiative heat loss from the Ge cell layer to the sky and $q_{conv,Ge\to a}$ is the convective heat loss from the Ge cell layer to the ambient.

The convective heat losses from the Ge layer to the ambient can be calculated using [12]:

$$q_{conv,Ge\to a} = h_{conv,wind}\left(T_{Ge} - T_a\right) \tag{15}$$

$$h_{conv,\,wind} = 5.82 + 4.07V_{wind} \tag{16}$$

where, T_a is the ambient temperature, T_{Ge} is the temperature of the Germanium cell, V_{wind} is the wind velocity, and $h_{conv,wind}$ is the convective heat transfer coefficient.

The radiative heat losses from the Ge layer to the sky can be calculated using [12]:

$$q_{rad,Ge\to S} = \sigma\epsilon_{Ge}(T_{Ge}^4 - T_s^4) \tag{17}$$

$$T_s = 0.0522T_a^{1.5} \tag{18}$$

where, ε_{Ge} is the emissivity of Ge, and T_s denotes the sky temperature in Kelvin.

At the interfaces between solar cell, DBC assembly, heat sink and TEG:

$$-k_m\nabla T_m = -k_n\nabla T_n \; and \; T_m = T_n \tag{19}$$

At the heat sink inlet: $V_f = V_{in}$ and $T_{in} = 298$K

At heat sink outlet: gauge pressure $P_{out} = 0$

No slip boundary condition is given at the fluid-solid interface.

5. Results and Discussion

The current study investigates the effect of confined jet impingement cooling combined with a thermoelectric generator on the performance of the HCPV-T system. A 25 × 25 mm aluminium heat sink and a TEG are placed at the backside of the solar PV cell and copper-ceramic assembly. The upper surface of the PV cell and the upper copper layer are subjected to convective and radiative boundary conditions. All sides of the PV cell, DBC assembly, and heat sink are subjected to convective boundary conditions. The interfaces of all the layers are given thermally coupled boundary conditions.

5.1 Validation of the numerical model:

The current numerical model is validated with the results obtained by Abo-Zahhad et al. The authors studied the effect of a confined jet impingement cooling system on the performance of the HCPV-T system. Figure 2(a) depicts the validation of the solar cell model with the results obtained by Abo-Zahhad et al. [6] with a maximum error of 1.8%. Figure 2 (b) shows the validation of the TEG model with the datasheet as provided by the manufacturer [14]. It can be observed that the TEG model predicts electric power generation with less than 6% error in the temperature range of 80 °C to 110 °C. However, the thermophysical properties and the Seeback coefficient of the TEG are assumed to be constant in the current study. This leads to an increase in errors at the high temperature of the TEG hot junction, increasing the difference between the current study and experimental data to around 11% in the temperature range of 120 °C to 140 °C.

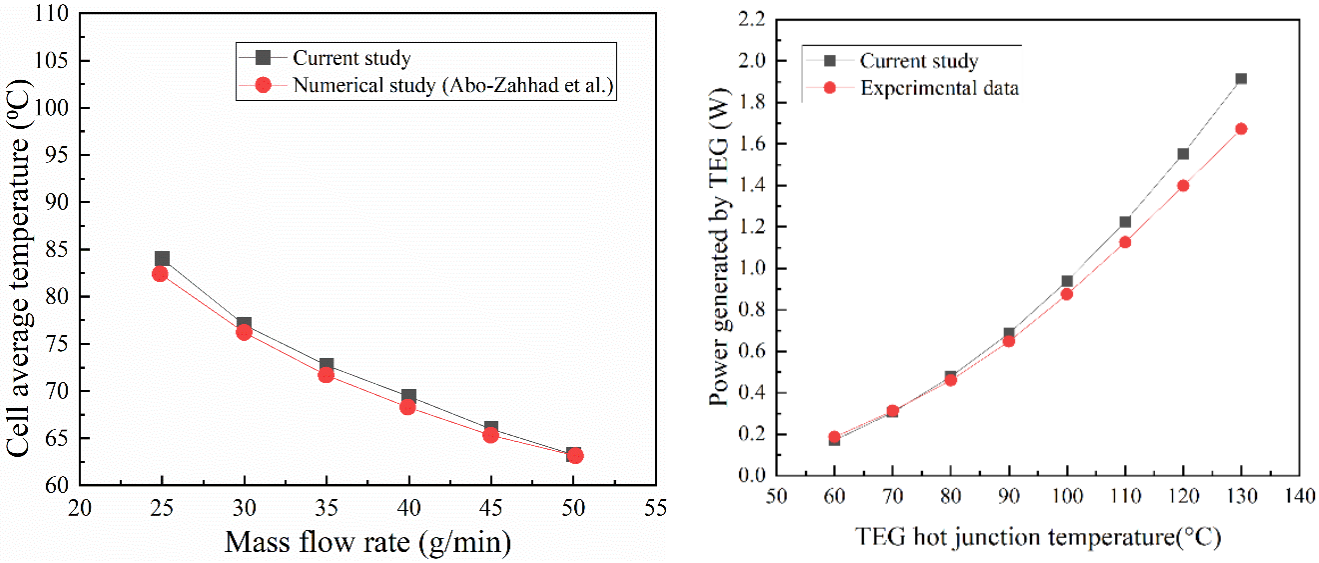

Figure 2. Validation of (a) solar cell model, (b) TEG model

5.2 Variation in cell average temperature and cell electrical efficiency:

Figure 3(a) shows the variation in cell average temperature with ṁ for three distinct TEG sizes at CR = 1000. The cell average temperature is 87.8 °C, 95.66 °C, 129.8 °C at $\dot{m}$ = 25 g/min, which decreases to 73.4 °C, 80.9 °C, 115 °C at $\dot{m}$ = 50 g/min for TEG sizes of 15 × 15 mm, 20 × 20 mm, and 25 × 25 mm respectively. It can be observed that cell average temperature decreases with an increase in ṁ due to an increase in heat transfer coefficient at higher ṁ. The cell temperature increases with an increase in the TEG area. As the TEG area increases, less heat is conducted from the PV cell to the aluminium heat sink due to the lower thermal conductivity of TEG material. The lower thermal conductivity of the TEG module leads to a high thermal resistance. Hence, only a small portion of the heat generated in the PV cell is cooled by the

confined jet impingement cooling system. This leads to an increase in the temperature of the PV cell. It can be observed that the PV cell temperature increases sharply with the 25 × 25 mm TEG module. The 25 × 25 mm TEG module covers the entire heat sink top surface. It leads to a very high thermal resistance between the bottom copper layer and the aluminium heat sink, leading to a sharp increase in the PV cell temperature.

Figure 3(b) shows the variation in cell electrical efficiency with $\dot{m}$ for three distinct TEG sizes at CR = 1000. The cell electrical efficiency is 38%, 37.6%, and 36% at $\dot{m}$ = 50 g/min for TEG sizes 15 × 15 mm, 20 × 20 mm, and 25 × 25 mm, respectively. The cell electrical efficiency is a function of cell temperature. Hence, the cell electrical efficiency decreases with an increase in the average temperature of the cell. The open circuit voltage of the PV cell reduces with an increase in cell temperature, leading to a decrease in cell electrical efficiency.

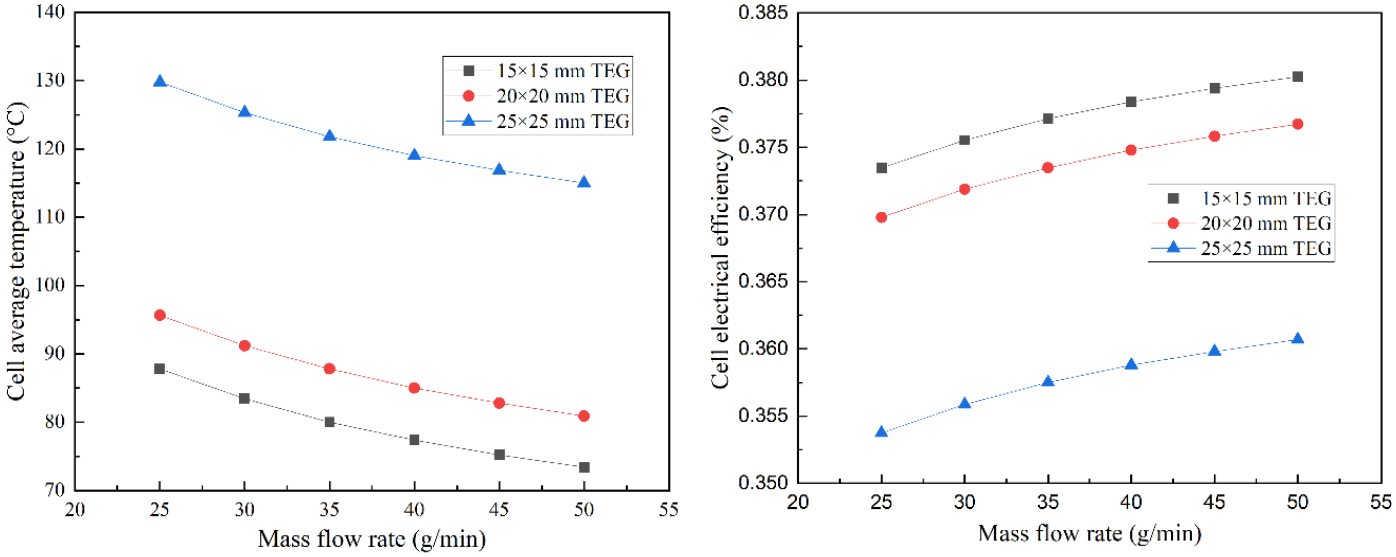

(a) (b)

Figure 3. Variation in (a) cell average temperature, (b) cell electrical efficiency with coolant mass flow rate at CR = 1000

5.3 Effect of TEG area on total power generation:

Figure 4(a) shows the variation in electrical power generated by the TEG modules with $\dot{m}$ at CR = 1000. The electrical power generated by the TEG module is 0.27 W, 0.28 W, 4.25 W at $\dot{m}$ = 25 g/min, which reduces to 0.46 W, 0.47 W, 1.76 W at $\dot{m}$ = 50 g/min for TEG sizes 15 × 15 mm, 20 × 20 mm, and 25 × 25 mm respectively. The temperature difference between hot and cold junctions of the TEG module reduces with an increase in $\dot{m}$ due to increased heat transfer coefficient at higher mass flow rates. The electrical power generation by the TEG module is directly proportional to the temperature difference between hot and cold junctions. This leads to a decrease in electrical power generation by the TEG module at higher $\dot{m}$. The temperature between the hot and cold junction of the TEG is higher with the 25 × 25 mm TEG module. Hence, the electrical power generated by the 25 × 25 mm TEG module is higher than the 20 × 20 mm and 15 × 15 mm TEG modules.

Figure 4(b) shows the electrical power generated by the PV cell, TEG module, and the total electrical power generation by the hybrid system for the different TEG sizes at $\dot{m}$ = 25 g/min at CR = 1000. The power generated by the PV cell is 29.57 W, 29.28 W, and 28.01 W for TEG sizes of 15 × 15 mm, 20 × 20 mm, and 25 × 25 mm, respectively. The total electrical power generated by the hybrid system is 29.84 W, 29.56 W, and 32.27 W for TEG sizes 15×15 mm, 20×20 mm, and 25×25 mm, respectively. The power generated by the PV cell decreases with an increase in TEG area due to reduced cell electrical efficiency. The cell temperature increases with an increase in TEG area, resulting in reduced cell electrical efficiency. However, the electrical power generated by the TEG module increases with an increase in the TEG area. The electrical resistance of the TEG module decreases with an increased temperature of hot and cold junctions of TEG. This results in an increased electric current in the TEG module. This leads to an increase in power generation by the TEG module at high

temperatures of hot and cold junctions of the TEG module. It can be observed that the total power generated by the hybrid system slightly decreases initially, with an increase in TEG area from 15 × 15 mm to 20 × 20 mm. The electrical power generated by the 20 × 20 mm TEG module is not able to compensate for the electrical power loss from the PV cell. It is also observed that the total power generated by the hybrid system increases for the 25 × 25 mm TEG module. The electrical power generated by the PV cell is reduced with the 25 × 25 mm TEG module. However, the electrical power generated by the 25 × 25 mm TEG module is high, resulting in a high electrical power output from the hybrid system.

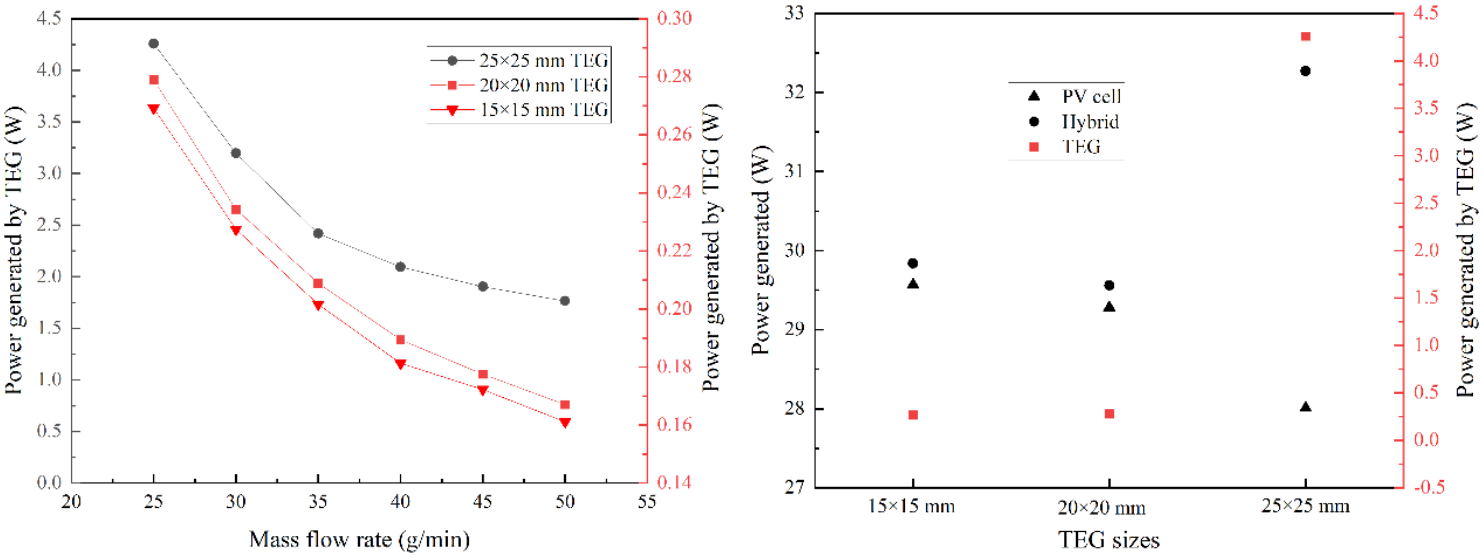

Figure 4. Variation in (a) TEG power generation with coolant mass flow rate, (b) power generation with TEG sizes at $\dot{m}$ = 25 g/min and CR = 1000

6. Conclusions

The current study evaluates the effect of hybrid cooling consisting of confined jet impingement and thermoelectric generators on the performance of the HCPV-T system. The performance of the HCPV-T system is studied with three distinct TEG module sizes. The average temperature of the PV cell increases with an increase in the area of the TEG module. This leads to a decrease in cell electrical efficiency of the PV cell. However, the electrical power generated by the TEG module increases with an increased area of the TEG module as a result of increased temperature difference between hot and cold junctions of the TEG modules. The electrical resistance of the TEG module decreases with an increased temperature of hot and cold junctions of TEG, which results in an increased electrical current in the TEG module. Hence, the total electrical power generated by the hybrid cooling system increases with the 25 × 25 mm TEG module. The total electrical power generated by the hybrid system is 29.84 W, 29.56 W, and 32.27 W for TEG sizes of 15 × 15 mm, 20 × 20 mm, and 25 × 25 mm, respectively. However, the maximum temperature of the solar cell goes beyond the permissible temperature limit of 110 °C with the 25 × 25 mm TEG module as a result of high thermal resistance between the bottom copper layer and the aluminium heat sink. Hence, the channel design for the confined jet impingement has to be optimised in such a way that the PV cell temperature reduces below 110 °C by maintaining a high-temperature difference between hot and cold junctions of the TEG module. The study of the optimum channel design for the hybrid system will be performed in future numerical studies.

References

[1] P. Dwivedi, K. Sudhakar, A. Soni, E. Solomin, and I. Kirpichnikova, “Advanced cooling techniques of P.V. modules: A state of art,” *Case Stud. Therm. Eng.*, vol. 21, no. December 2019, p. 100674, 2020.

[2] M. Theristis and T. S. O'Donovan, "Electrical-thermal analysis of III-V triple-junction solar cells under variable spectra and ambient temperatures," *Sol. Energy*, vol. 118, pp. 533–546, 2015.
[3] A. Royne and C. J. Dey, "Design of a jet impingement cooling device for densely packed PV cells under high concentration," *Sol. Energy*, vol. 81, no. 8, pp. 1014–1024, 2007.
[4] M. Javidan and A. J. Moghadam, "Experimental investigation on thermal management of a photovoltaic module using water-jet impingement cooling," *Energy Convers. Manag.*, vol. 228, no. October 2020, 2021.
[5] H. M. S. Bahaidarah, "Experimental performance evaluation and modeling of jet impingement cooling for thermal management of photovoltaics," *Sol. Energy*, vol. 135, pp. 605–617, 2016.
[6] E. M. Abo-Zahhad, S. Ookawara, A. Radwan, A. H. El-Shazly, and M. F. ElKady, "Thermal and structure analyses of high concentrator solar cell under confined jet impingement cooling," *Energy Convers. Manag.*, vol. 176, no. August, pp. 39–54, 2018.
[7] J. Tang, X. Li, R. Hu, Z. Mo, and M. Du, "A novel designed manifold ultrathin micro pin-fin channel for thermal management of high-concentrator photovoltaic system," *Int. J. Heat Mass Transf.*, vol. 183, 2022.
[8] A. Shohdy, M. Emam, H. Sekiguchi, and H. Hassan, "Performance of new hybrid heat sink with trimmed fins and microchannels for thermal control of a triple-junction concentrator photovoltaic cell," *Appl. Therm. Eng.*, vol. 252, no. February, 2024.
[9] M. Sabry, A. Lashin, and M. Al Turkestani, "Experimental and simulation investigations of CPV/TEG hybrid system," *J. King Saud Univ. - Sci.*, vol. 33, no. 2, p. 101321, 2021.
[10] H. R. Fallah Kohan, F. Lotfipour, and M. Eslami, "Numerical simulation of a photovoltaic thermoelectric hybrid power generation system," *Sol. Energy*, vol. 174, no. July, pp. 537–548, 2018.
[11] "3C44A – with 10×10 mm2Concentrator Triple Junction Solar cell. http://www. azurspace.com 2016:1–6."
[12] A. Aldossary, S. Mahmoud, and R. Al-Dadah, "Technical feasibility study of passive and active cooling for concentrator PV in harsh environment," *Appl. Therm. Eng.*, vol. 100, pp. 490–500, 2016.
[13] A. Bitschi, "Modelling of thermoelectric devices for electric power generation," no. 18441, p. 144, 2009.
[14] Https://customthermoelectric.com/1261g-7l31-04cqthermoelectric- and Generator-40-x-40mm.html., "Commercial TEG 1261G-7L31-04CQ data sheet, manufactured by Custom Thermoelectric,."